

Incident-energy and polarization dependent RIXS study of La_2CuO_4

L. Lu,¹ J. N. Hancock,² G. Chabot-Couture,¹ K. Ishii,³ O. P. Vajk,⁴ G. Yu,⁵ J. Mizuki,³ D. Casa,⁶ T. Gog,⁶ and M. Greven^{1,2}

¹*Department of Applied Physics, Stanford University, Stanford, California 94305*

²*Stanford Synchrotron Radiation Laboratory, Stanford, California 94309*

³*Synchrotron Radiation Research Unit, Japan Atomic Energy Agency, Hyogo 679-5148, Japan*

⁴*NIST Center for Neutron Research, National Institute of Standards and Technology, Gaithersburg, Maryland 20899*

⁵*Department of Physics, Stanford University, Stanford, California 94305*

⁶*CMC-XOR, Advanced Photon Source, Argonne National Laboratory, Argonne, Illinois 60439*

(Dated: October 30, 2018)

We present a detailed Cu K -edge resonant inelastic X-ray scattering (RIXS) study of the Mott insulator La_2CuO_4 in the 1-7 eV energy transfer range. As initially found for the high-temperature superconductor $\text{HgBa}_2\text{CuO}_{4+\delta}$, the spectra exhibit a multiplet of weakly-dispersive electron-hole excitations, which are revealed by utilizing the subtle dependence of the cross section on the incident photon energy. The close similarity between the fine structures for in-plane and out-of-plane polarizations is indicative of the central role played by the $1s$ core hole in inducing charge excitations within the CuO_2 planes. On the other hand, we observe a polarization dependence of the spectral weight, and careful analysis reveals two separate features near 2 eV that may be related to different charge-transfer processes. The polarization dependence indicates that the $4p$ electrons contribute significantly to the RIXS cross section. Third-order perturbation arguments and a shake-up of valence excitations are then applied to account for the final-energy resonance in the spectra. As an alternative scenario, we discuss fluorescence-like emission processes due to $1s \rightarrow 4p$ transitions into a narrow continuum $4p$ band.

PACS numbers: 74.25.Jb, 74.72.-h, 78.70.Ck, 71.35.-y

I. INTRODUCTION

With the advent of 3rd generation synchrotron sources, inelastic X-ray scattering has emerged as a powerful probe of momentum and energy-dependent charge and lattice dynamics. This development has led to new insight into low-density metallic electrodynamics [1], valence fluctuating compounds [2], H_2O molecular correlations [3, 4], phonon dynamics [5], and the Mott physics of correlated electron systems such as the lamellar copper oxides [6, 7, 8, 9, 10, 11, 12, 13, 14] and the manganites [15, 16]. Resonant inelastic X-ray scattering (RIXS) provides a considerable advantage over ordinary inelastic scattering since, at resonance, the inelastic signal is significantly enhanced [17]. In the lamellar copper oxides, this resonance condition can be readily met by tuning the incoming photon energy to the vicinity of the Cu K edge. The RIXS cross section sensitively depends on the incident photon energy and on the nature of the intermediate states [12, 18, 19, 20].

The intermediate state of the Cu K -edge RIXS process is the same as the final state of X-ray absorption: a localized core hole is created through $1s \rightarrow 4p$ photoexcitation. The $1s$ core hole interacts strongly with the valence electron system, generating a strong response that corresponds to the many-electron bound states of the local, nascent core-hole potential [21]. In RIXS, the eventual relaxation of these highly excited states leads to the emission of photons, leaving the valence system in an excited state. One usually identifies energy-loss features with the excitations of the valence electrons. When viewed as

a second-order optical process, there exists a close connection between the initial absorption and final emission stages in RIXS. Accordingly, the spectra simultaneously depend on both the incident and final photon energies [22].

In the present work, we investigate these energy dependences, as well as the polarization dependence, in the best-characterized lamellar copper oxide: La_2CuO_4 . This Mott insulator is the parent compound of the original high-temperature superconductor $(\text{La},\text{Ba})_2\text{CuO}_4$, and it has been the subject of a number of prior RIXS studies [10, 12, 23]. Exploiting the incident-energy sensitivity, we are able to identify new charge excitation features. We demonstrate that the fine structure is present for photon polarizations both parallel and perpendicular to the CuO_2 planes, and suggest that the subtle differences between the two polarization conditions can be explained in terms of models in which the $4p$ electrons play a significant role.

This paper is organized as follows: after the discussion of the experimental details in the next Section, we present our results for out-of-plane and in-plane polarization in Sections III and IV, respectively. Section V contains a discussion of our data, and we summarize our work in Section VI.

II. EXPERIMENTAL DETAILS

The focus of this work is on the collective electronic excitations of La_2CuO_4 in the 1-7 eV range using incident

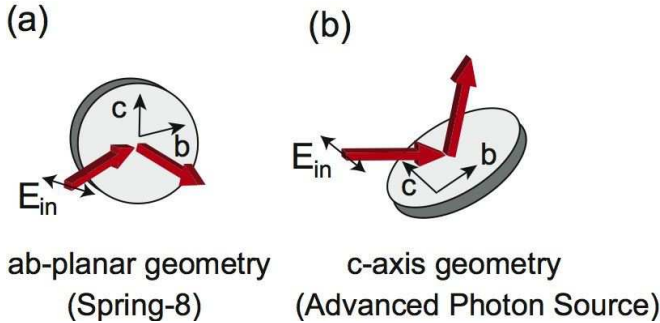


FIG. 1: The two scattering geometries used in this study and discussed in the text.

photon energies in the vicinity of the Cu K -edge absorption threshold. We have measured the RIXS response at several high-symmetry positions in the Brillouin zone, covering a fine mesh of incident and scattered photon energies around the Cu K edge.

Two sets of measurements were taken, one collected at the Advanced Photon Source with incident photon polarization vector perpendicular to the CuO₂ planes ($\mathbf{E} \parallel c$), and the other at SPring-8 (Japan) with incident photon polarization parallel to the CuO₂ planes ($\mathbf{E} \perp c$). The measurements with in-plane polarization [Fig. 1 (a)] were taken in horizontal scattering geometry at beam line BL11XU at SPring-8, with the tetragonal reciprocal lattice point $\mathbf{G}=(3,0,0)$ as Brillouin zone center, and a scattering angle of $\sim 65^\circ$. A Si(111) main monochromator and a Si(400) secondary monochromator were used to obtain an incident energy resolution of 220 meV. A bent Ge(733) analyzer crystal situated at the end of a 2 m four-circle diffractometer arm selected the energy of the photons scattered from the sample, which were then collected by a solid state detector. In this geometry, the polarization vector of the incident photon was always parallel to the CuO₂ planes, with a typical angle of $\sim 32^\circ$ with respect to the tetragonal a axis, i.e., the planar Cu-O bond direction. The overall energy resolution was about 400 meV (FWHM), as determined from the energy width of the elastic line.

Out-of-plane polarization measurements [Fig. 1 (b)] were performed at beam line 9-ID-B at the Advanced Photon Source in a vertical scattering geometry. The reciprocal lattice vectors (3,0,0) and (1,0,0) were chosen as reference zone centers, because Bragg scattering at these locations is forbidden, to reduce the contribution from the elastic tail. The set-up employed a Si(111) primary monochromator, a Si(333) secondary monochromator, and a spherical diced Ge(733) analyzer crystal with a 1 m radius, and yielded an overall energy resolution of about 300 meV (FWHM). For data that were measured at the reduced wave vector $(\pi,0)$, or absolute momentum of $(1.5,0,0)$, we used a primary Si(111) and a second Si(444) channel-cut monochromator with a 2 m arm. This configuration can provide at best an energy

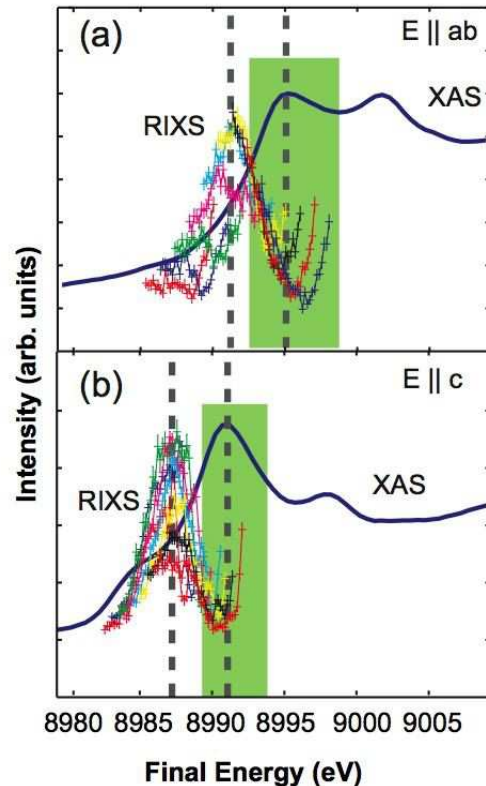


FIG. 2: RIXS spectra plotted versus final photon energy along with the absorption spectra monitored by total fluorescence yield for photons polarized (a) parallel and (b) perpendicular to the CuO₂ planes. The shaded areas indicate the incident-energy ranges probed in the present study. All spectra were taken at $\mathbf{Q} = (3,0,0)$ and at different incident energies corresponding to the shaded ranges.

resolution of 110 meV, but we chose wide aperture slits in front of the detector to obtain a resolution of ~ 300 meV for better comparison with measurements at other wave vectors.

Both data sets were taken at ambient temperature on the same single-crystalline sample. La₂CuO₄ undergoes a tetragonal-to-orthorhombic structural phase transition at ~ 530 K associated with the staggered tilting of the CuO₆ octahedra [24]. We note that our crystal is twinned, and hence we do not distinguish between the two inequivalent planar orthorhombic directions. The crystal was grown in an image furnace at Stanford University. As-grown crystals are known to contain excess oxygen, and hence hole carriers. In order to assure that our sample was free of any carriers it was annealed for 24 h in Ar flow at 950° C. This reduction treatment resulted in a Néel temperature of $T_N \sim 320$ K, as determined from a measurement of the magnetic susceptibility [25].

Figure 2 shows the X-ray absorption spectra (XAS) for each polarization condition as measured by total fluorescence yield. For each polarization, there are two peaks: 8991 and 8998 eV for $\mathbf{E} \parallel c$, and 8995 and 9002 for $\mathbf{E} \perp c$.

The lower of these resonances is usually identified with a transition into a “well-screened state” [6, 8, 10], a many-body excitation which effectively screens the $1s$ core hole and has significant $1s4p3d^{10}L$ character. The higher resonance is identified with a transition into a “poorly-screened state” [6, 8, 10], another bound state of the many-electron system in the core hole potential which has predominantly $1s4p3d^9$ character. For each polarization, the resonance peaks are separated by approximately 7 eV. The resonance energies differ by about 4 eV between the two geometries, which may be primarily due to the larger Cu-O distance for the negatively charged apical oxygens, rendering the $4p_z$ electronic orbitals lower in energy than their $4p_\sigma$ counterparts [26, 27]. The spectra presented in this paper were taken in the vicinity of the “well-screened” condition for both polarization geometries.

III. INCIDENT ENERGY DEPENDENCE, OUT-OF-PLANE POLARIZATION

RIXS spectra obtained in early work in the soft X-ray regime exhibited a clear incident and final photon energy dependence [22]. The incident-photon-energy dependence was recently utilized in the hard X-ray regime (at the Cu K edge) in both La_2CuO_4 and in the single-layer high-temperature superconductor $\text{HgBa}_2\text{CuO}_{4+\delta}$ (Hg1201) [12]. This study revealed new features in the 2-5 eV range, an observation that necessitates a new interpretation of the charge dynamics in these materials. For example, a ~ 2 eV feature was identified in Hg1201. It was argued in Ref. [12] that this feature is not likely a $d \rightarrow d$ excitation, but rather that it indicates the presence of a remnant charge-transfer gap even at optimal doping in this model superconductor. The presence of an additional feature at ~ 3 eV, which was only identified through inspection of multiple spectra with different incident photon energies, constrains the dispersion of the 2 eV feature to be less than 500 meV. The same approach was applied to La_2CuO_4 , and preliminary data revealed charge-transfer features that are remarkably similar to those in Hg1201 [12], a result that is qualitatively different from prior work on the Mott insulators La_2CuO_4 [10] and $\text{Ca}_2\text{CuO}_2\text{Cl}_2$ [9]. The small dispersion of the 2 eV feature was further confirmed by subsequent measurements [23, 28]. Our primary focus here is to investigate in greater detail the incident-energy and polarization dependence of the inelastic cross section near the absorption threshold in La_2CuO_4 .

The molecular orbital excitation at ~ 7 eV was studied in detail in Ref. [11] and is most prominently observed near $E_i = 8998$ eV, an incident photon energy for which the lower-lying charge-transfer excitations in the 2-6 eV range do not resonate. We therefore limit our attention to the incident energy range $E_i = 8989$ -8994 eV [shaded area in Fig. 2 (a)] and to energy transfers below 7 eV for out-of-plane polarization. A fine step size of $\Delta E_i = 500$

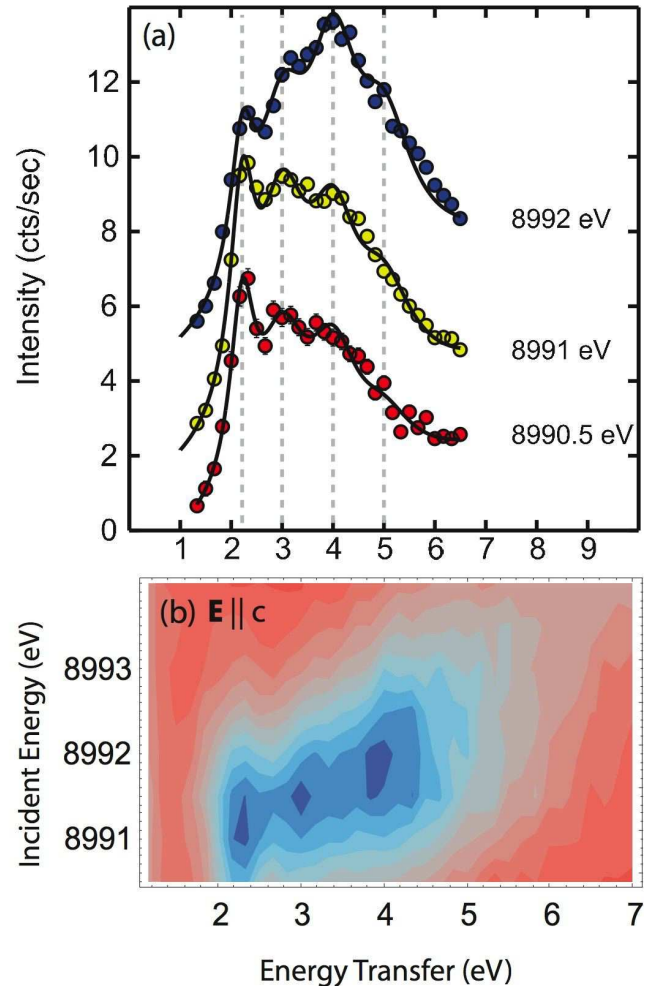


FIG. 3: (a) RIXS signal versus energy transfer for out-of-plane polarization at three representative incident energies at a momentum transfer of $(3,0,0)$, which corresponds to the two-dimensional zone center $(0,0)$. The lines are the result of a fit, as discussed in the text (reproduced from [12]). (b) Contour plot of all zone-center scans, taken in 500 meV increments of E_i .

meV was chosen, allowing us to demonstrate the high sensitivity of the RIXS cross section to the incident photon energy.

Figure 3 (a) shows representative line scans at the zone center, taken at three different incident photon energies with out-of-plane polarization. These data resemble previous work [10], yet closer inspection reveals additional features. The most distinct feature is that at ~ 2 eV. As the incident energy is increased, this sharp feature gradually weakens relative to those at higher energy. Another new feature at 3 eV, which was not observed in prior work [10], can be discerned at all three incident photon energies. The feature at ~ 4 eV, also seen in previous zone-center data [10], becomes dominant at $E_i = 8992$ eV. Finally, a comprehensive analysis of all data [12] reveals a second

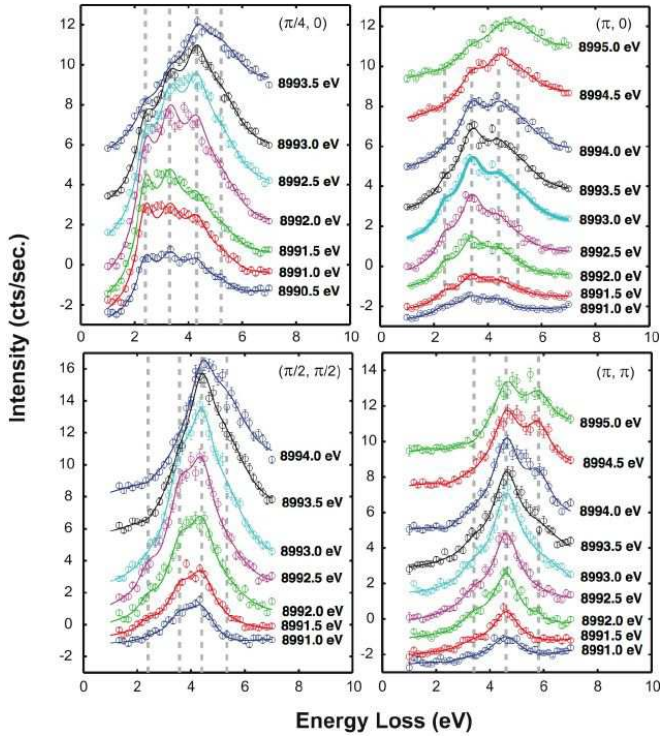


FIG. 4: Incident-energy dependence of the $\mathbf{E}||c$ RIXS spectra for (a) $(\pi/4, 0)$, (b) $(\pi, 0)$, (c) $(\pi/2, \pi/2)$, (d) (π, π) . The lines are the result of fits, as discussed in the text.

new feature at ~ 5 eV. As discussed in detail below, the systematic center-of-mass shift with incident energy suggests a strong modulation of the inelastic cross-section by the final photon energy.

Figure 3 (b) shows a contour plot constructed from all line scans at the zone center. This mode of representation is similar to the “RIXS plane” of incident photon energy versus energy transfer in Ref. [29]. By extending the energy-transfer spectra into the incident-energy dimension, features at ~ 2.3 , 3 and 4 eV are readily apparent.

Figure 4 shows additional results at high-symmetry points of the two-dimensional Brillouin zone. Using the fit procedure defined in Ref. [12], the spectra at each momentum transfer are fit simultaneously to obtain the peak positions that determine the energy transfer of the corresponding charge excitations. Specifically, we assume that the peak positions do not vary with incident energy and that each feature is represented by a Lorentzian line shape. The number, energy-transfer positions and energy widths of the features are considered to be shared parameters for all spectra at the same momentum transfer. At different incident energies, on the other hand, the spectral weight of each component is allowed to vary. We also use spectra on the energy gain-side for background subtraction, and allow for linear slopes to approximate

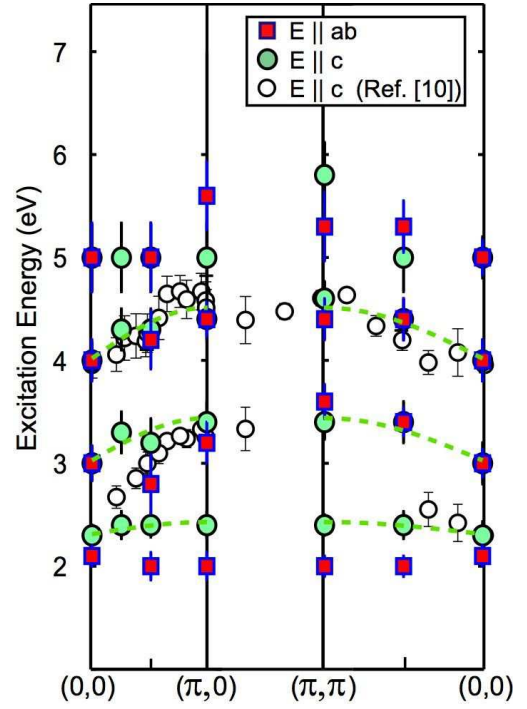


FIG. 5: Dispersion of the charge excitations for both in-plane and out-of-plane polarization along the two high-symmetry directions studied in the present work. The dashed lines indicate sinusoidal fits to the dispersion of the three lowest-energy features discerned with out-of-plane polarization. Previous results [10], obtained with out-of-plane polarization, are shown for comparison.

the continuum due to transitions to continuous unoccupied states. A simultaneous least-squares fit of all spectra results in the lines in Figs. 3 (a) and 4, and allowed us to extract the peak positions plotted in Fig. 5.

Although the different components are not as easily distinguishable as at the zone center, the relative strengths of the four features identified below 6 eV exhibit a clear dependence on momentum transfer and incident energy, which suggests that the corresponding excitations have different symmetries. The 5 eV component is visually resolvable only at (π, π) and at relatively high incident energies. Away from the zone center, the relative weight of the 2 eV feature quickly decreases. While the 2 eV and 3 eV features are still separable and comparable in strength at $(\pi/4, 0)$, the 2 eV component is only barely visible (at low incident energies) at $(\pi, 0)$. On the other hand, the 3 eV and 4 eV features maintain comparable weight along $[\pi, 0]$. In contrast, along $[\pi, \pi]$, the overall response away from the zone center appears to be dominated by the (approximately Lorentzian-shaped) response just above 4 eV. As for the fine structure, the momentum dependence away from the zone center is again consistent with what is observed in Hg1201, although that study was carried out with in-plane polarization [12].

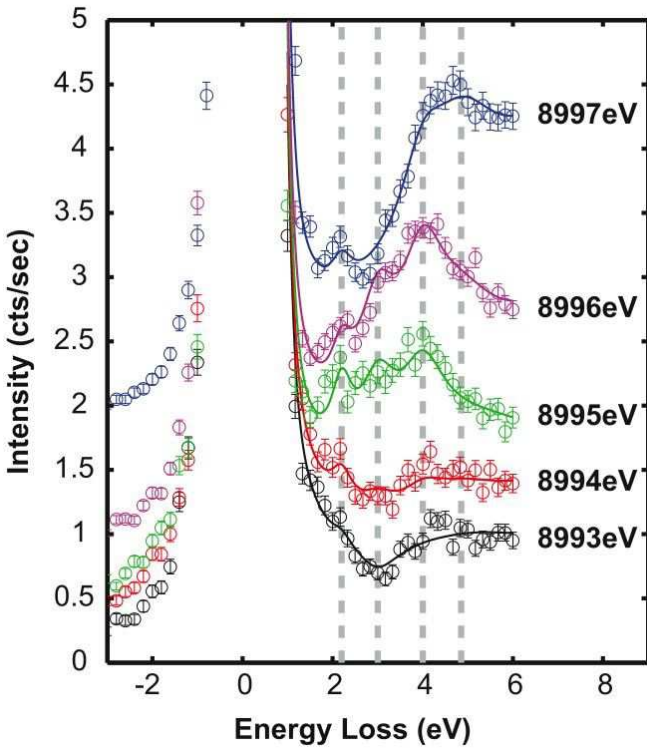


FIG. 6: Five line scans at the zone center obtained with in-plane polarization.

IV. INCIDENT ENERGY DEPENDENCE, IN-PLANE POLARIZATION

Figure 6 shows line scans at the zone center for the complementary in-plane-polarized (SPring-8) experiment. As indicated in Fig. 2 (b), the incident photon energy was chosen to lie in the range 8993 - 8999 eV. The fine structure revealed through the incident energy dependence of the spectra is very similar to that of the out-of-plane polarized experiment. Although there exist differences in intensity between the two experiments, the absolute magnitude is not directly comparable due to many differences in the experimental configurations. Overall, there are still four major peaks present at ~ 2 , 3 , 4 and 5 eV. The close similarity of the spectra supports the intuitive notion that the spherically-symmetric $1s$ core hole potential dominates the generation of the valence excitations in both cases [9, 30, 31, 32, 33].

There also exist similarities between the two polarization geometries in the momentum dependence of the multiplet structure. Figure 7 shows line scans with fits at four reduced momentum transfer values away from the zone center. As in the out-of-plane polarized experiment, the strength of the 2 eV feature decreases toward the zone boundary. In the present case, it is no longer visually observable at $(\pi, 0)$. Also, the 3 eV and 4 eV features have comparable spectral weight throughout the Brillouin zone along $(\pi, 0)$, and are still equivalent up to

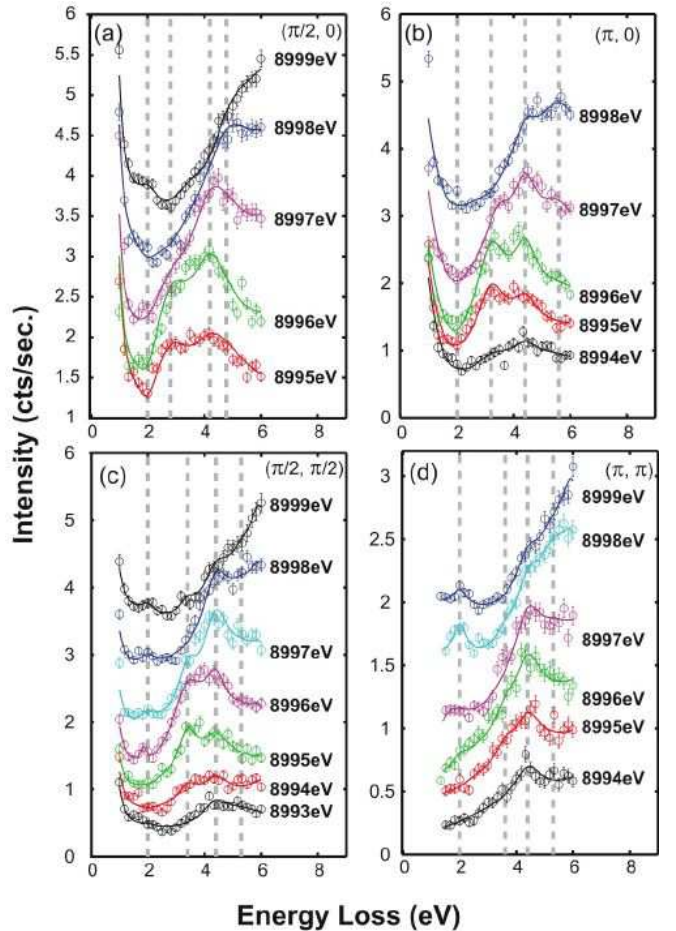


FIG. 7: RIXS spectra with $\mathbf{E}||ab$ at (a) $(\pi/2, 0)$ (b) $(\pi, 0)$ (c) $(\pi/2, \pi/2)$, and (d) (π, π) .

$(\pi/2, \pi/2)$ along (π, π) . However, the 3 eV feature is quickly suppressed between $(\pi/2, \pi/2)$ and (π, π) and, as for out-of-plane polarization, the 4 eV spectral weight becomes dominant.

Differences between two polarizations are also noticeable. First, with in-plane polarization approximately along $[1, 1, 0]$, the relative intensity of 2 eV feature with respect to spectral features with higher energy transfer is much weaker than that for the out-of-plane polarized experiment. However, the 2 eV feature is still observable even up to (π, π) , reaching a maximum at an incident energy of 8997 eV, slightly above the absorption threshold (8995 eV) for in-plane polarization. Second, for in-plane polarization, as we increase in incident energy, the center of mass of the spectra continuously shifts to higher energy transfers. For c polarization, on the other hand, it peaks between 4 and 5 eV.

As for the $\mathbf{E}||c$ data, all spectra acquired at the same momentum transfer were simultaneously fit assuming the same set of peak positions. The results of the fits are shown by the lines in Figs. 6 and 7, and the peak positions are compared to those for out-of-plane polarization

in Fig. 5. While there is an overall good agreement, the 2 eV features have significantly different excitation energies for two the polarizations. We note that the dispersion of all four features summarized in Fig. 5 is weak. These observations will be discussed in more detail in the next Section.

V. DISCUSSION

The presence of a ~ 2 eV resonance feature has been discussed in connection with excitations across the charge transfer gap [7, 9, 10, 12, 22]. In La_2CuO_4 , this excitation is observed only for transitions into well-screened states, in which the $1s$ core hole is screened by a valence electron from a neighboring CuO_4 plaquette, leaving a doubly-occupied Cu^+ ion ($3d^{10}$) and a hole on the neighboring plaquette. It has been suggested that the non-local hole can form a Zhang-Rice singlet [34], which can propagate efficiently through the antiferromagnetic background, and that this singlet could form a strong bond with the Cu^+ quasi-particle and become even more dispersive as a bound exciton [35]. However, high-resolution electron-energy-loss spectroscopy (EELS) on the related Mott insulator $\text{Sr}_2\text{CuO}_2\text{Cl}_2$ suggests the existence of another charge-transfer excitation, with slightly lower energy, that involves only the local CuO_4 plaquette [36]. These findings were argued to be consistent with embedded molecular cluster calculations [36]. Indeed, our data reveal that the excitation energies for in-plane and out-of-plane polarizations differ by as much as 300 meV. While the former excitation has no discernible dispersion, the latter appears to disperse by 100-150 meV toward the zone boundary. In addition to these differences, we also find that the spectral weights of these two low-energy features exhibit rather different momentum dependences, especially along $[\pi, \pi]$. We note that it is not likely that the 2 eV features are $d \rightarrow d$ excitations, since the latter lie below 2 eV and are expected to be much weaker at the K edge than at the L and M edges [12].

In an attempt to understand the differences between the two 2 eV features, we consider a possible photon polarization effect. When the polarization vector of the incident photon lies within the CuO_2 plane, the $4p$ electron in the intermediate state is in the $4p_\sigma$ orbital [see Fig. 8 (b)] and overlaps with the $2p_{x,y}$ electrons. The repulsive Coulomb interaction between $\text{O} 2p$ and $\text{Cu} 4p$ therefore tends to suppress the $\text{O}2p \rightarrow \text{Cu}3d$ charge transfer. On the other hand, for out-of-plane polarization, the $4p_z$ electron is oriented in the direction that is orthogonal to that of the $2p_{x,y}$ electrons [see Fig. 8 (c)] and the Coulomb interaction has a limited effect on the charge-transfer process. That difference in intermediate states may explain why we observe a second (local) “2eV” component for in-plane polarization, since the component that involves a non-local charge transfer process from neighboring CuO_4 plaquette to central core hole site could be spectroscopically suppressed for in-plane polar-

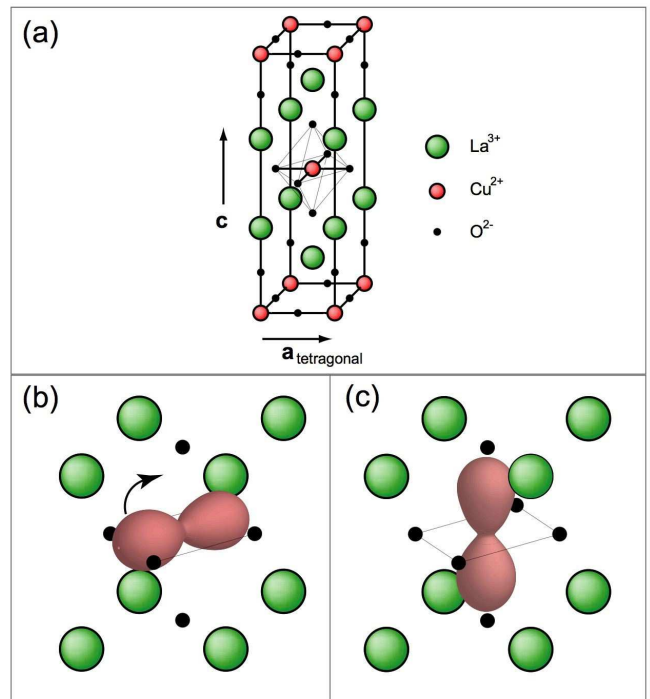


FIG. 8: (a) La_2CuO_4 unit cell. In a $\text{Cu} K$ -edge absorption process, several $4p$ states can be reached, depending on the polarization of the incident photon relative to the crystal axes. (b) $4p_\sigma$ configuration created by absorption of a $E_i \sim 8996$ eV photon with $E \parallel ab$. (c) $4p_z$ configuration created by absorption of a $E_i \sim 8991$ eV photon with $E \parallel c$. The emissive process discussed in the text corresponds to relaxation from state (b) to state (c).

ization. The lower of the two “2 eV” features may be intrinsically weaker, which could explain why we are unable to discern it for out-of-plane polarization. The above is consistent with earlier suggestions based on $\text{Cu} K$ -edge XAS [37]. Especially for in-plane polarization, the low-energy excitation still maintains its strength along (π, π) , whereas it is weakened at the same location for out-of-plane polarization. Therefore, it indeed appears that these two low-energy excitations have a distinct physical origin, consistent with the high-resolution EELS work [36].

The magnitude of the dispersion will be an important factor in the eventual determination of the origin of the charge excitations. Our La_2CuO_4 data reveal charge-transfer features that are remarkably similar to those for $\text{Hg}1201$ [12], a result that is qualitatively different from prior work on La_2CuO_4 [10]. As summarized in Figure 5, below 4 eV we identify one additional branch at ~ 3 eV for both polarizations. From simple fits to a sinusoidal form, e.g. for out-of-plane polarization, we obtain dispersions of 120(30), 410(110), and 490(70) meV for the 2, 3, and 4 eV features along both high-symmetry directions. The 5 eV feature appears to be dispersion-

less, with the exception of a possible anomaly at (π, π) . Below, we discuss the possibility that the 5 eV feature may actually be the result of a “shake-up” excitation at 7.2 eV. The ~ 100 meV dispersion of the non-local 2 eV excitation is less than the Zhang-Rice singlet bandwidth of 250 meV, identified by angular resolved photoemission spectroscopy [38, 39, 40]. This observation challenges the notion of an excitonic picture to explain the dispersion of the charge-transfer gap excitation. In principle, if the electron and hole are asymmetric [41], the observed dispersion may either represent the bandwidth of the UHB, if the electron is more mobile, or of the Zhang-Rice singlet band, if the hole is more free to move. However, it is difficult to reconcile the small electron-hole-pair dispersion of ~ 100 meV with the relatively large Zhang-Rice singlet bandwidth, unless the observed behavior represents a significant core-hole effect.

In order to understand the appearance of multiple charge excitations in the higher energy (transfer) region, a more complex approach appears to be necessary. An initial suggestion concerning the 4 eV excitation invoked an excitonic state of unspecified origin [10], yet more recent theoretical work [12, 32, 42] suggests that the higher-energy spectral features ought to be described in terms of a multi-band picture. Considering the involvement of bonding and nonbonding oxygen $2p_\sigma$ and $2p_z$ orbitals, as well as charge-transfer processes through local and nonlocal screening channels, there exist many candidate modes. Eskes and Sawatzky [43] also find that triple-band physics, including the Zhang-Rice triplet states, as well as $d_{3z^2-r^2}$ -orbitals are relevant up to about 7 eV in binding energy. Further experimentation, including symmetry analysis, is required to resolve the physical origin of the high-energy spectral features.

We will now discuss the photon energy and polarization dependence of these higher-energy features. Figure 9 (a) shows zone-center contour plots of incident energy versus energy transfer. The out-of-plane data are from Ref. [10], which were taken with coarser incident energy step size (1 eV vs. 0.5 eV) but span a wider incident energy range than our data in Fig. 3 (b). The in-plane data (inset) are from our present study and were taken with incident energy increments of 1 eV. As mentioned above, the center of mass of the RIXS spectra shifts to higher energy transfer as the incident photon energy increases. This variation is identified in Fig. 9 (a) as a “streak” of intensity from 2 to 7 eV which, instead of extending horizontally as one would expect for resonances associated with fixed incident photon energy, tilts toward the upper-right corner. We will first discuss that this streak of intensity can be interpreted in a “shake-up” picture, which uses third-order perturbation theory. As an alternative scenario for the slope-one component of this streak of intensity between ~ 5 and 7 eV, we will then discuss fluorescence-like emission processes due to $1s \rightarrow 4p$ transitions into a narrow continuum $4p$ band.

Pioneering work on La_2CuO_4 [7] utilized in-plane polarization and revealed one single excitation between \sim

3 and 6 eV, and it was found that the peak position varied nonlinearly with incident energy. These results were interpreted in terms of a shake-up of the $3d$ electron system, and explained within third-order perturbation theory. Following this qualitative treatment, which was formulated in detail in Ref. [7, 19, 44], the scattering amplitude in third-order perturbation theory is given by

$$A \propto \sum_{m,n} \frac{\langle f|b_2|m\rangle\langle m|H_c|n\rangle\langle n|b_1|i\rangle}{(E_m - E_{f,el} - E_f - i\Gamma_m)(E_n - E_{i,el} - E_i - i\Gamma_n)} \approx \frac{\langle f|b_2H_c b_1|i\rangle}{(E_{ex,2} - E_f - i\Gamma_2)(E_{ex,1} - E_i - i\Gamma_1)} \quad (1)$$

where $|m\rangle$ and $|n\rangle$ denote different intermediate states containing a virtual $1s4p$ exciton, E_i and E_f are the incident and final photon energies, $E_{i,el}$ and $E_{f,el}$ the initial energy and final energies of the electron system, and b_1 and b_2 are absorption and emission operators [19]. A simplification is made by defining the constants $E_{ex,1} \equiv E_n - E_{i,el}$, and $E_{ex,2} \equiv E_m - E_{f,el}$, which can be considered incident and final resonant energies, respectively, and the respective inverse lifetimes Γ_1 and Γ_2 [7, 19]. With this simplification, we ignore the details of the intermediate states. We note that this formula contains separate denominators involving incident and final photon energies. The scattering intensity is given by

$$I \sim L(E_{ex,1} - E_i, \Gamma_1) L(E_{ex,2} - E_f, \Gamma_2) \times |\langle f|b_2H_c b_1|i\rangle|^2 \delta(E_{f,el} - E_{i,el} - \omega), \quad (2)$$

where $L(E, \Gamma_i)$ represents a Lorentzian function with half width Γ_i .

To model the shake-up process, we replace $|\langle f|b_2H_c b_1|i\rangle|^2$ with a sum of Gaussian functions, each representing a distinct symmetry-allowed shake-up excitation with energy Δ and heuristic inverse life-time Γ_s :

$$G(\omega) = \exp\left(-\frac{(\omega - \Delta)^2}{2\Gamma_s^2}\right). \quad (3)$$

The single excitation observed in prior work on La_2CuO_4 [7] was described with $\Gamma_1 = \Gamma_2 = 2.38$ eV, $E_{ex,1} = E_{ex,2} = 8995$ eV, $\Gamma_s = 3.9$ eV and $\Delta = 6.1$ eV. Since we have been able to resolve a multiplet of excitations rather than a single excitation, we apply third-order perturbation theory to the entire multiplet. In our calculation, we find that four valence excitations with energies $\Delta = 2.3, 3, 4$ and 7.2 eV are adequate to represent the spectra for both polarizations. The result of this calculation is shown in Fig. 9 (b). For this particular calculation, we chose Γ_s to be 0.4, 1.0, and 1.1 eV for the lower three excitations, respectively. We find that our data can be adequately represented if the 7.2 eV molecular orbital excitation resonates for transitions into both well- and poorly-screened states, with variable characteristics. This excitation is represented by two Gaussians

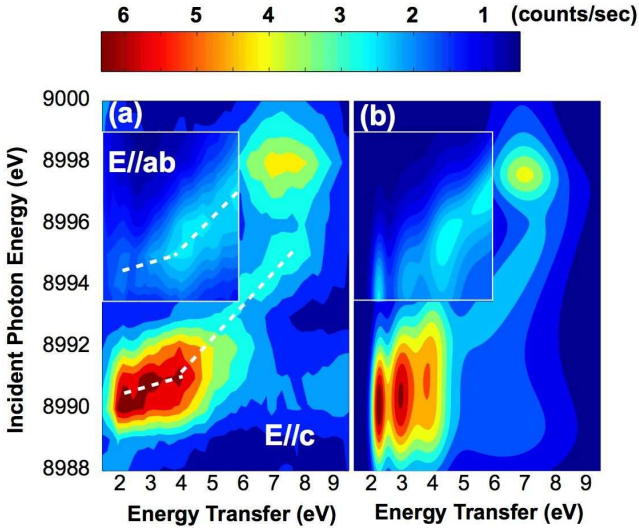


FIG. 9: (Color) (a) Contour plot of La_2CuO_4 RIXS intensity: incident photon energy vs. energy transfer for $E \parallel c$ (from Ref. [10]) and $E \parallel ab$ (inset; present work). The white dashed lines indicate the two trends with different slope, as discussed in the text. (b) Calculations following third-order perturbation theory, as discussed in the text.

(with Γ_s set to 3.9 eV (well-screened) and 1.9 eV (poorly screened)), and we consider a total of five Gaussians for four excitations.

We note that the 5 eV feature discussed in Sections III and IV was not considered in the above calculations since it is most prominent at high incident energies and shifts with E_i . It therefore seems likely that this feature may actually be associated with a resonance of the 7.2 eV molecular orbital excitation at the well-screened state. Due to the double-resonance denominator, each component may, in principle, show two separate resonances for $E_i = E_{ex,1}$ and $E_f = E_{ex,2}$. For the final-energy resonance, as the incident energy changes, the peak position of the excitation shifts to $\omega_{peak} = E_i - E_{ex,2}$ so as to maintain the same final energy. In the two-dimensional contour plot of Fig. 9, this manifests itself as a slope-one streak of intensity.

The inverse lifetimes determine the shapes of the resonant spectral features. When Γ_1 , Γ_2 , and Γ_s approach the value of excitation energy Δ , the two resonances merge and become indistinguishable. If Γ_1 or Γ_2 is small compared to Δ and Γ_s , one of the two resonances nearly disappears, and the response either is a circular region or a slope-one streak. By carefully choosing Γ_i and $E_{ex,i}$ ($i = 1, 2$) for each component, we were able to emulate the main characteristics of the experimental data. As seen from Fig. 9 (a), the lowest three excitations are only strongly resonant at the well-screened state, while the 7.2 eV excitation is associated with the poorly-screened state. Consequently, E_{ex} should be different for the latter. For the slope-one streak component, the incident resonance energy is the same as for the lower three ex-

citations, but we find it necessary to choose a slightly smaller $E_{ex,2}$. The differing effects of the electrons in the $4p_z$ and $4p_\sigma$ orbitals on the charge-transfer processes within the CuO_2 plane require separate spectral weight components for the two polarization conditions.

Specifically, for out-of-plane polarization, we set $\Gamma_1 = \Gamma_2 = 2$ eV and $E_{ex,1} = E_{ex,2} = 8990$ eV for the lower three excitations. For the 7.2 eV component that results in the diagonal streak, we set $\Gamma_1 = 1.7$ eV, $\Gamma_2 = 1.5$ eV, $E_{ex,1} = 8990$ eV, and $E_{ex,2} = 8989$ eV, and for the other 7.2 eV component we chose $\Gamma_1 = 1.0$ eV, $\Gamma_2 = 1.5$ eV and $E_{ex,1} = E_{ex,2} = 8998.5$ eV. For in-plane polarization, we simply shifted all E_{ex} values by 4 eV, and adjusted the relative intensity between the three low-lying excitations and the two 7.2 eV components.

The above analysis has two important implications. One is that the “5 eV” feature is to be viewed as a shake-up excitation at 7.2 eV. The second important implication is that this local molecular-orbital excitation not only resonates at the poorly screened state at which copper has an open-shell configuration ($1s3d^94p$), but also at the well-screened state ($1s3d^{10}4p$). This is different from findings for CuO and from the argument that the observed shake-up excitation requires the $3d^9$ open-shell configuration and should be absent at the well-screened state [19]. However, we note that the molecular-orbital excitation was observed to be resonant at both well-screened and poorly-screened states in superconducting $\text{HgBa}_2\text{CuO}_{4+\delta}$ [12].

We will now discuss a different interpretation for the slope-one component of the streak of intensity that relates it to a resonant excitation into the continuum of unoccupied states [45, 46]. Figure 2 shows the zone-center RIXS spectra together with the respective absorption spectra for both polarizations. The RIXS intensity is plotted versus final photon energy (E_f) instead of energy transfer (ω). We find that the spectra collapse to a peak, with an envelope of approximately Lorentzian shape, centered at about $E_f = 8991$ eV for in-plane polarization and $E_f = 8987$ eV for out-of-plane polarization. The peak position lies ~ 4 eV below the photoabsorption threshold for both polarizations. This observation is consistent with the presence of slope-one streaks in the contour plots for both polarizations: for in-plane polarization this streak starts at $E_i \sim 8995$ eV and for out-of-plane polarization it starts at $E_i \sim 8991$ eV.

As is well known, the electronic states in the cuprates have either local or extended character. The photon-absorption process near the Cu K -edge is comprised of transitions to either narrow molecular orbitals or continuum unoccupied states. For discrete levels, such as the “well-screened” and “poorly-screened” states, induced valence excitations resonate and follow the Raman-Stokes law as E_i crosses the discrete levels, i.e., the excitational energies Δ do not vary with incident photon energy. On the other hand, a resonance due to transitions to continuum states behaves differently. Here, the resonance condition is fulfilled for every incident energy

tuned to the continuum, and the subsequent emission is independent of E_i once the incident energy increases above the lower edge of the continuum. When E_i is below the edge, the resonant emission should also follow the Raman linear dispersion, but the spectral weight may be suppressed due to the small density of states below the edge. Our observation suggests that there may exist a continuous unoccupied band of $4p$ symmetry, with an edge at ~ 8991 eV and ~ 8995 eV for the respective polarizations, and a width of about 3-4 eV. This supports the view that a combination of an extended picture of itinerant $4p$ electrons and of localized molecular orbitals is necessary to interpret the K -edge absorption spectra [21] and the nature of the intermediate states in RIXS.

We note that the envelope of the in-plane data collapse in Fig. 2 (a) is very similar in shape and position to the XAS peak corresponding to the well-screened state for out-of-plane polarization. This leads us to another interpretation of the slope-one contribution to the RIXS cross section shown in Fig. 9 (a). Specifically, it suggests that part of the in-plane-polarized RIXS signal can be interpreted through the following complex dynamical process illustrated in Fig. 8: La_2CuO_4 absorbs a photon of energy $E_i \sim 8995$ eV with polarization $\mathbf{E} \perp c$, creating on a Cu site a well-screened 1s core hole and an electron in a $4p_\sigma$ orbital [Fig. 8 (b)]. The $4p_\sigma$ electron then evolves into a $4p_z$ state [Fig. 8 (c)] via a subsequent relaxation process. Finally, the $4p_z$ electron recombines with the 1s core hole, emitting a photon with energy ~ 8991 eV. However, for out-of-plane polarization, electrons are already excited into a $4p_z$ state, and this relaxation will not occur. Nevertheless, the envelope for out-of-plane polarization lies also 4eV below that of the main edge. This interpretation therefore requires the existence of a discrete lower-energy state with energy 8987 eV for $4p_z$ electron to relax into. Interestingly, in Ref. [7], a resonance of approximately this energy was observed with

in-plane polarization.

VI. SUMMARY

In summary, we have presented a detailed Cu K -edge RIXS study of La_2CuO_4 in which we resolve a multiplet of charge-transfer excitations in the 1-7 eV range. We suggest several interpretations to explain the polarization-dependent spectra. A calculation applying third-order perturbation theory introduces a final-energy resonance and successfully simulates the main characteristics of the spectra for both polarizations. On the other hand, transitions to continuum $4p$ bands that begin at the main absorption edge as well as $4p_\sigma \rightarrow 4p_z$ relaxation are offered as alternative explanations to the fluorescence-like component in the contours. These proposals all emphasize the important role of the $4p$ electrons in the RIXS cross section.

VII. ACKNOWLEDGEMENTS

The authors gratefully acknowledge valuable discussions with P. Abbamonte, U. Bergmann, J. van den Brink, T. P. Devereaux, M. V. Klein, Y. J. Kim, K.-W. Lee, R. S. Markiewicz, W. E. Pickett, K. M. Shen, M. van Veenendaal, and F. C. Zhang. The work at Stanford University was supported by the DOE under Contract Nos. DE-FG03-99ER45773 and DE-AC03-76SF00515. Work at the CMC-XOR Beamlines is supported in part by the Office of Basic Energy Sciences of the U.S. Dept. of Energy and by the National Science Foundation Division of Materials Research. Use of the Advanced Photon Source is supported by the Office of Basic Energy Sciences of the U.S. Department of Energy under Contract No. W-31-109-Eng-38

[1] C. A. Burns, P. Abbamonte, E. D. Isaacs, and P. M. Platzman, Phys. Rev. Lett. **83**, 2390 (1999).
[2] C. Dallera, M. Grioni, A. Shukla, G. Vanko, J. L. Sarrao, J. P. Rueff, and D. L. Cox, Phys. Rev. Lett. **88**, 196403 (2002).
[3] P. Wernet, D. Nordlund, U. Bergmann, M. Cavalleri, M. Odelius, H. Ogasawara, L. A. Naslund, T. K. Hirsch, L. Ojamae, P. Glatzel, L. G. M. Pettersson, and A. Nilsson, Science **304**, 995 (2004).
[4] F. Sette, G. Ruocco, M. Krisch, U. Bergmann, C. Masiccio, V. Mazzacurati, G. Signorelli, and R. Verbeni, Phys. Rev. Lett. **75**, 850 (1995).
[5] M. d'Astuto, P. K. Mang, P. Giura, A. Shukla, P. Ghigna, A. Mirone, M. Braden, M. Greven, M. Krisch, and F. Sette, Phys. Rev. Lett. **88** (2002).
[6] J. P. Hill, C. C. Kao, W. A. L. Caliebe, M. Matsubara, A. Kotani, J. L. Peng, and R. L. Greene, Phys. Rev. Lett. **80**, 4967 (1998).
[7] P. Abbamonte, C. A. Burns, E. D. Isaacs, P. M. Platzman, L. L. Miller, S. W. Cheong, and M. V. Klein, Phys. Rev. Lett. **83**, 860 (1999).
[8] K. Hämäläinen, J. P. Hill, S. Huotari, C. C. Kao, L. E. Berman, A. Kotani, T. Ide, J. L. Peng, and R. L. Greene, Phys. Rev. B **61**, 1836 (2000).
[9] M. Z. Hasan, E. D. Isaacs, Z. X. Shen, L. L. Miller, K. Tsutsui, T. Tohyama, and S. Maekawa, Science **288**, 1811 (2000).
[10] Y. J. Kim, J. P. Hill, C. A. Burns, S. Wakimoto, R. J. Birgeneau, D. Casa, T. Gog, and C. T. Venkataraman, Phys. Rev. Lett. **89** (2002).
[11] Y. J. Kim, J. P. Hill, S. Komiya, Y. Ando, D. Casa, T. Gog, and C. T. Venkataraman, Phys. Rev. B **70** (2004).
[12] L. Lu, X. Zhao, G. Chabot-Couture, J. N. Hancock, N. Kaneko, O. P. Vajk, G. Yu, S. Grenier, Y. J. Kim, D. Casa, T. Gog, and M. Greven, Phys. Rev. Lett. **95**, 217003 (2005).
[13] K. Ishii, K. Tsutsui, Y. Endoh, T. Tohyama, S. Maekawa,

M. Hoesch, K. Kuzushita, M. Tsubota, T. Inami, J. Mizuki, Y. Murakami, and K. Yamada, Phys. Rev. Lett. **94**, 207003 (2005).

[14] K. Ishii, K. Tsutsui, Y. Endoh, T. Tohyama, K. Kuzushita, T. Inami, K. Ohwada, S. Maekawa, T. Masui, S. Tajima, Y. Murakami, and J. Mizuki, Phys. Rev. Lett. **94**, 919 (2005).

[15] K. Ishii, T. Inami, K. Ohwada, K. Kuzushita, J. Mizuki, Y. Murakami, S. Ishihara, Y. Endoh, S. Maekawa, K. Hirota, and Y. Moritomo, Phys. Rev. B **8**, 224437 (2004).

[16] S. Grenier, J. P. Hill, V. Kiryukhin, W. Ku, Y. J. Kim, K. J. Thomas, S. W. Cheong, Y. Tokura, Y. Tomioka, D. Casa, and T. Gog, Phys. Rev. Lett. **94** (2005).

[17] C. C. Kao, W. A. L. Caliebe, H. J. B, and J. M. Gillet, Phys. Rev. B **54**, 16361 (1996).

[18] M. H. Krisch, C. C. Kao, F. Sette, W. A. Caliebe, K. Hämäläinen, and J. B. Hastings, Phys. Rev. Lett. **74**, 4931 (1995).

[19] G. Döring, C. Sternemann, A. Kaprolat, A. Mattila, K. Hämäläinen, and W. Schulke, Phys. Rev. B **70**, 085115 (2004).

[20] P. Glatzel and U. Bergmann, Coord. Chem. Rev. **249**, 65 (2005).

[21] J. M. Tranquada, S. M. Heald, W. Kunnmann, A. R. Moodenbaugh, S. L. Qiu, Y. W. Xu, and P. K. Davies, Phys. Rev. B **44**, 5176 (1991).

[22] A. Kotani and S. Shin, Rev. Mod. Phys. **73**, 203 (2001).

[23] E. Collart, A. Shukla, J. P. Rueff, P. Leininger, H. Ishii, I. Jarrige, Y. Q. Cai, S. W. Cheong, and G. Dhaleen, Phys. Rev. Lett. **96**, 157004 (2006).

[24] R. J. Birgeneau, M. Greven, M. A. Kastner, Y. S. Lee, B. O. Wells, Y. Endoh, K. Yamada, and G. Shirane, Phys. Rev. B **59**, 13788 (1999).

[25] O. P. Vajk, P. K. Mang, M. Greven, P. M. Gehring, and J. W. Lynn, Science **295**, 1691 (2002).

[26] S. M. Heald, J. M. Tranquada, A. R. Moodenbaugh, and Y. W. Xu, Phys. Rev. B **38**, 761 (1988).

[27] K.-W. Lee and W. E. Pickett, Private Communication (2006).

[28] Y. J. Kim, private communication (2006).

[29] P. Glatzel and U. Bergmann, Coord. Chem. Rev. **249**, 65 (2005).

[30] G. D. Mahan, *Many-Particle Physics* (Springer Verlag, New York, 2000).

[31] F. deGroot, Chem. Rev. **101**, 1779 (2001).

[32] T. Nomura and J. Igarashi, Phys. Rev. B **71**, 035110 (2005).

[33] K. Tsutsui, T. Tohyama, and S. Maekawa, Phys. Rev. Lett. **91** (2003).

[34] F. C. Zhang and T. M. Rice, Phys. Rev. B **37**, 3759 (1988).

[35] F. C. Zhang and K. K. Ng, Phys. Rev. B **58**, 13520 (1998).

[36] A. S. Moskvin, R. Neudert, M. Knupfer, J. Fink, and R. Hayn, Phys. Rev. B **65**, 180512 (2002).

[37] H. Tolentino, M. Medarde, A. Fontaine, F. Baudelet, E. Dartyge, D. Guay, and G. Tourillon, Phys. Rev. B **45**, 008091 (1992).

[38] B. O. Wells, Z. X. Shen, A. Matsuura, D. M. King, M. A. Kastner, M. Greven, and R. J. Birgeneau, Phys. Rev. Lett. **74**, 964 (1995).

[39] C. Dürr, S. Legner, R. Hayn, S. V. Borisenko, Z. Hu, A. Theresiak, M. Knupfer, M. S. Golden, J. Fink, F. Ronning, Z.-X. Shen, H. Eisaki, S. Uchida, C. Janowitz, R. Müller, R. L. Johnson, K. Rossnagel, L. Kipp, and G. Reichardt, Phys. Rev. B **63**, 014505 (2000).

[40] F. Ronning, C. Kim, K. M. Shen, N. P. Armitage, A. Damascelli, D. H. Lu, D. L. Feng, Z.-X. Shen, L. L. Miller, Y. J. Kim, F. Chou, and I. Terasaki, Phys. Rev. B **67**, 035113 (2003).

[41] K. H. Ahn, A. J. Fedro, and M. van Veenendaal, cond-mat/0412635 (2004).

[42] R. S. Markiewicz and A. Bansil, Phys. Rev. Lett. **96**, 107005 (2006).

[43] H. Eskes and G. Sawatzky, Phys. Rev. B **44**, 9656 (1991).

[44] P. M. Platzman and E. D. Isaacs, Phys. Rev. B **57**, 11107 (1998).

[45] F. Gel'Mukhanov and H. Ågren, Phys. Rev. B **57**, 2780 (1998).

[46] F. Gel'Mukhanov and H. Ågren, Phys. Rep. **312**, 87 (1999).